

A Depth-Aware Swap Insertion Scheme for the Qubit Mapping Problem

Chi Zhang* Yanhao Chen† Yuwei Jin†
Wonsun Ahn* Youtao Zhang* Eddy Z. Zhang†

*University of Pittsburgh
{chz54, wahn}@pitt.edu, zhangyt@cs.pitt.edu

†Rutgers University
chenyh64@gmail.com, yj243@scarletmail.rutgers.edu, eddy.zhengzhang@gmail.com

Abstract—The rapid progress of physical implementation of quantum computers paved the way of realising the design of tools to help users write quantum programs for any given quantum devices. The physical constraints inherent to the current NISQ architectures prevent most quantum algorithms from being directly executed on quantum devices. To enable two-qubit gates in the algorithm, existing works focus on inserting SWAP gates to dynamically remap logical qubits to physical qubits. However, their schemes lack the consideration of the depth of generated quantum circuits. In this work, we propose a depth-aware SWAP insertion scheme for qubit mapping problem in the NISQ era.

Index Terms—Quantum Computing, Emerging languages and compilers, Emerging Device Technologies

I. INTRODUCTION

Quantum computing has exhibited its theoretical advantage over classical computing by showing impressive speedup on applications including large integer factoring [1], database search [2], and quantum simulation [3]. It is considered to be a new computational model that may have a subversive impact on the future, and has attracted major interests of a large number of researchers and companies.

With the advent of advanced manufacturing technology, the industry is able to build small-scale quantum computers – Noisy Intermediate-Scale Quantum [4] (NISQ) devices. A NISQ device is equipped with dozens to hundreds of qubits. IBM [5] released its 53-qubit quantum computer in October 2019 and has made it available for commercial use. Google [6] released the 72-qubit *Bristlecone* quantum computer in March 2018. Other companies including Intel [7], Rigetti [8], and IonQ, have released their quantum computing devices with dozens of qubits. The current NISQ technology may not be perfect, but it’s a good first step towards the more powerful quantum devices in the future.

In order to map high level quantum programs to NISQ devices, it is important to overcome two obstacles. First, to be able to execute a quantum circuit, it is necessary to map logical qubits to physical qubits with respect to architecture and program coupling constraints. Any quantum program can be implemented using an universal gate set [9] of a small number of elementary gates. For instance, the $\{H, CNOT, S, T\}$ set is an universal gate set, in which the $\{H, S, T\}$ gates are single qubit gates, the *CNOT* gate is a two-qubit gate.

The two-qubit gate must be mapped to two qubits that are physically connected. However, in real quantum architecture, qubits may have limited connection and not every two qubits are connected, as shown in the IBM *QX2* architecture in Fig. 1 (a). For this reason, a quantum circuit is not directly executable on a NISQ device, unless circuit transformation is performed. The common practice is to insert *SWAP* operations to dynamically remap the logical qubit such that the transformed circuit is hardware-compliant for each (set of) two-qubit gate(s).

Second, it is critical that the depth of a quantum circuit be minimized for the NISQ device. A qubit is volatile and error prone. It gradually decays over time and may have phase and bit flip errors. It may completely lose its state after a certain period of time, called *coherence time*. Quantum error correction (QEC) codes can detect error syndromes and fix them. However, QEC needs to use a large number of redundant physical qubits. A realistic QEC circuit may need more than 10,000 physical qubits, which is not possible for today’s NISQ device. Without QEC, a program must terminate within a threshold amount of time. The depth of the circuit, which is the number of steps the circuit executes, must be optimized. IBM proposed the metric of *quantum volume* [10] for evaluating the effectiveness of quantum computers which accounts for not only the width of the circuit (the number of qubits), but also the depth, how many steps the circuit can execute.

Transforming the logical circuit into a hardware-compliant one will inevitably result in increased gate count and circuit depth. Most previous work for qubit mapping [11]–[16] focus on minimizing the number of inserted gates, but not the depth of the transformed circuit. However, even if the gate count is small, it does not necessarily mean the depth of the circuit is small, due to the dependence between different gates. We discover that previous work that aims to minimize number of inserted gate may significantly increase the depth of the circuit (in Section IV). For instance, the Sabre approach by Li *et al.* [11] reduces the gate count by 1.1%, but increases the depth of the 10-qubit *QFT* circuit by over 44.5%. The two studies [17], [18] stress the importance of taking into consideration the variability in the qubit (link) error rates, but they do not directly address the issue of the increased circuit depth.

The depth of the circuit, as mentioned above, is critical and

determines if a quantum program is executable on a NISQ device with respect to its physical limits. In this paper, we propose the first depth-aware qubit mapping scheme for quantum circuits running on arbitrary qubit connectivity hardware. Our depth-aware qubit mapper searches for the mapping that minimizes the transformed circuit depth and keeps the gate count within a reasonable range. Our results show we can reduce the depth of the transformed circuit by up to 30% compared with two best known qubit mappers [11], [12], and in the meantime, have on average less than 3% additional gates over a large set of representative benchmarks.

II. BACKGROUND AND MOTIVATION

A. Quantum Computing Basics

1) *Qubit*: A quantum bit or qubit, is the counterpart to classical bit in the realm of quantum computing. Different from a classical bit that represents either ‘1’ or ‘0’, a qubit is in the coherent superposition of both states. It is considered as a two-state quantum system that exhibits the peculiarity of quantum mechanics [9]. An example is the spin of the electron that the two states can be spin up and spin down.

2) *Quantum Gates*: There are two types of basic quantum gates. One type of basic gates is the single-qubit gate, a unitary quantum operation that can be abstracted as the rotation around the axis of the Bloch sphere [9] which represents the state space of one qubit. A single qubit-gate can be parameterized using two rotation angles around the axes. There are several elementary single-qubit gates including the Hadamard (H) gate, the phase (S) gate, and the $\pi/8$ (T) gate [9]. The other type of basic gates is the multi-qubit gate. However, all complex quantum gates can be decomposed into a sequence of single qubit gates H, S, T, and the two-qubit CNOT gate. Thus we only focus on the two-qubit CNOT gate. The CNOT gate operates on two qubits which are distinguished as a control qubit and a target qubit. If the control qubit is 1, the CNOT gate flips the state of the target qubit, otherwise, the target qubit remains the same.

3) *Quantum Circuit*: Quantum circuit is composed of a set of qubits and a sequence of quantum operations on these qubits. There are various ways to describe the quantum circuits. One way is to use the quantum assembly language called OpenQASM [19] released by IBM. Another way is to use the circuit diagram, in which qubits are represented as horizontal lines and quantum operations are the different blocks on those lines. In Fig. 2 (a), we show a simple example of quantum circuit diagram. A single-qubit gate is denoted as a square on the line, and one CNOT gate is represented by a line connecting two qubits and a circle enclosing a plus sign.

B. Qubit Mapping and Depth-Awareness

To enable the execution of a quantum circuit, the logical qubits in the circuit must be mapped to the physical qubit on the target hardware. When applying a CNOT gate, the two qubits connected by the CNOT gate need to be physically connected to each other. Due to the irregular physical qubit layout of existing devices, it is generally considered impossible

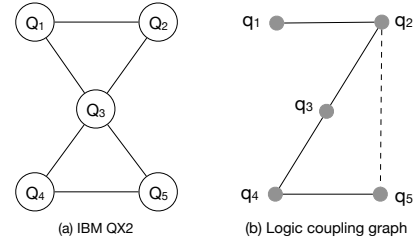


Fig. 1. (a) The connectivity structure of IBM QX2, (b) The coupling graph for logical qubits in the motivation example in Fig. 2

to find an initial mapping that makes the entire circuit CNOT-compliant. The common practice is to insert SWAP operations to remap the logical qubits. A swap operation exchanges the states of the two input qubits of interest. As shown in Fig. 3, a SWAP operation is implemented using 3 CNOT gates for architecture with bi-directional links, or 3 CNOT gates plus 4 Hadamard gates for architecture with single-direction links, where a bi-directional link means both ends of the link can be the control or target qubit, while single-direction link means only one end of it can be the control qubit.

IBM’s Qiskit uses a stochastic method to insert SWAPs [15] operations but often results in significant increase in the number of inserted gates and depth. Existing works [11], [14], [16] are more efficient than IBM’s Qiskit mapper. They use efficient heuristics to find the mapping rather than a stochastic method. However, the main objective of these methods is to reduce the gate count. It makes sense to minimize the gate count, but it is more important to focus on the depth of circuit, as in the NISQ era the depth is equivalent to the estimated execution time. Reducing the depth of the circuit can reduce the likelihood of the circuit failing at an early stage.

We show an motivation example in Fig. 2. The hardware model is shown in Fig. 1 (a). It has five qubits and the connectivity is the same as the IBM QX2 architecture except that the links are all bidirectional. There are 5 physical qubits: Q_1 to Q_5 and six bi-directional edges. One CNOT gate can only be applied on one of these edges.

In the example, the initial mapping between logical qubits (denoted by lower case q) and physical qubits (denoted by the upper case Q) is shown next to each qubit (line), which is $\{ \{q_1 \rightarrow Q_1\}, \{q_2 \rightarrow Q_2\}, \{q_3 \rightarrow Q_3\}, \{q_4 \rightarrow Q_4\}, \{q_5 \rightarrow Q_5\} \}$. With this initial mapping, it starts scheduling gates one by one until it encounters a (set of) CNOT gate(s) which cannot be scheduled due to physical constraints. We show the interaction of logical qubits in Fig. 1(b) such that two logical qubits are connected if there is a CNOT operation between them. When we encounter the gate “CNOT q_2, q_5 ” (marked red in the circuit diagram in Fig. 2 and as the dotted line in the logical coupling graph Fig. 1), the scheduling has to terminate since this translates into “CNOT Q_2, Q_5 ” on the hardware, while no physical link exists between Q_2 and Q_5 . Necessary SWAP operations are needed. When applying a SWAP operation, the two input physical qubits will exchange their

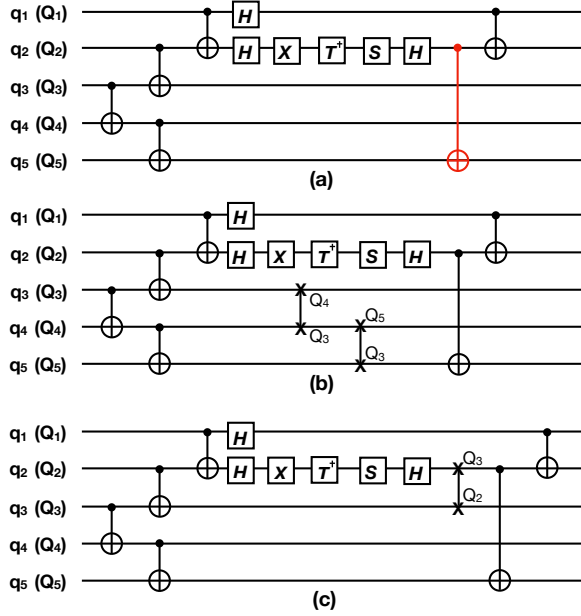


Fig. 2. Motivation Example: (a) the original logical circuit; (b) uses 2 swaps but the depth of the circuit is not increased; (c) only uses 1 swap but the depth of the circuit has been increased

states. Fig. 2 (b) and (c) provide two options for transforming the circuit. Fig. 2 (b) inserts 2 SWAPs (*SWAP* Q_3, Q_4 and *SWAP* Q_3, Q_5) such that “CNOT q_2, q_5 ” becomes “CNOT Q_2, Q_3 ”, however the two SWAPs can run in parallel with existing single qubit gates in the circuit, without having to increase the depth of the circuit. Fig. 2 (c) inserts only 1 SWAP (*SWAP* Q_2, Q_3) such that “CNOT q_2, q_5 ” becomes “CNOT Q_3, Q_5 ”, but it can not overlap with existing single-qubit gates in the circuit and will only increase the depth of the circuit by 3 (assuming we use 3 gates to implement the SWAP operation and each elementary gate takes 1 cycle in this example).

In this example, the best two known approaches by Zulehner *et al.* [14] and Li *et al.* [11] will both choose to insert 1 SWAP since they only optimize the number of gates inserted into the circuit (or the depth of the inserted gates), but not the depth of the entire transformed circuit. This example stresses the importance of depth-awareness in SWAP insertion schemes and motivates our work.

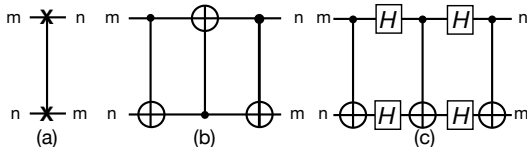


Fig. 3. Implementation of a SWAP operation

III. PROPOSED SOLUTION

A. Metric

As our work is a depth-aware SWAP insertion scheme, we first precisely define the metric for characterizing the depth

of a circuit. In order to fully explain the metric, we need to introduce the concepts of *dependency graph* and *critical path*.

The dependency graph represents the precedence relation between quantum gates in a logical quantum circuit. The definition is below:

Definition 1. Dependency Graph : *The dependency graph of a quantum circuit C with a set of gates Ψ is a Directed Acyclic Graph $G_\psi = (\Psi, E_\psi)$, $E_\psi \subseteq \psi \times \psi$. A directed edge from node ψ_1 to node ψ_2 exists if and only if the output of gate ψ_1 is (part of) the input of gate ψ_2 in the quantum circuit C .*

The critical path is referred to as the longest path in the dependency graph. And the definition is below:

Definition 2. Critical Path : *Given a dependency graph $G_\psi = (\Psi, E_\psi)$ of a quantum circuit. The critical path is $CP = \text{Max}(\text{Path}(\psi_1, \psi_2))$ s.t. $\psi_1, \psi_2 \in E_\psi$ and $\psi_1 \neq \psi_2$*

The depth is characterizing the number of execution steps of a quantum circuit, which is tantamount to the critical path length of the circuit. The longest path in the dependence graph describes the minimal number of steps the circuit needs in order for every gate’s data dependence be resolved. In Algorithm 1, we show how we calculate the critical path.

Algorithm 1: Calculate the Critical Path of a Circuit

Input : The circuit’s dependency graph $G(V, E)$

Output: The critical path CP

earliest_start = {};

CP = 0;

for $n \in V$ *in topological order* **do**

 temp = 0;

for $p \in V$ ’s predecessors **do**

if temp < earliest_start[p] + latency[p] **then**

 temp = earliest_start[p] + latency[p];

end

end

 earliest_start[n] = temp;

if CP < temp + latency[n] **then**

 CP = temp;

end

end

return CP ;

We first sort the nodes in the directed acyclic graph in topological order. Then we process the nodes in that order. For each node, we check the earliest start time for each of its predecessors, and add it by the latency of that predecessor, then we choose the maximum and use it as the earliest start time of this node. The maximum of all nodes’ earliest start time added by their latency is the critical path length.

We use the critical path length as the metric for ranking different swap insertion options.

B. Framework Design

With the metric precisely explained in previous section, now we continue to explain the work flow of our framework and

the intuitions behind it.

Before delving into the details of this framework, we need to define the *layer* and the *coupling graph*.

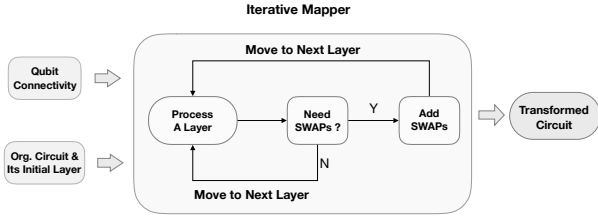


Fig. 4. The Qubit Mapping Framework

Definition 3. Coupling Graph : The coupling graph of a quantum architecture X with a set of physical qubits Q is a directed graph $G = (Q, E)$, $E \subseteq Q \times Q$. The edge $E_x = (Q_1, Q_2) \in E$ if and only if a CNOT gate can be applied to Q_1 and Q_2 in X with Q_1 being the control qubit and Q_2 being the target qubit.

We can divide the set of quantum gates in a circuit into layers, so that all gates in the same layer can be executed concurrently. The formal definition of a layer is:

Definition 4. Layer : A quantum circuit C can be divided into layers $L = l_1, l_2, l_3, \dots, l_m$, while $\bigcup_{i=1}^m l_i = C$ and $\bigcap_{i=1}^m l_i = \emptyset$. The set of gates at layer l_i can run concurrently and act on distinct sets of qubits.

To divide a circuit into layers, we group the gates that have the same *earliest start time* (defined in Algorithm 1) into the same layer. The order of the layers is thus determined by the order of the *earliest start times*.

We use an iterative process to find the mapping. Our framework is depicted in Fig. 4. And this iterative process is explained as below. We start the framework by taking the input of the coupling graph (also denoted as *Qubit Connectivity*) and the original circuit's initial layer.

We process the circuit layer by layer. Given a layer, we perform the following steps.

- We check the layer to see if it is hardware-compliant based on the coupling graph and the qubit mapping before current layer is scheduled.
- If YES, we move on to next layer.
- If NO, we invoke our mapping searcher to search for (the set of) swaps that are necessary to solve the current layer. We consider depth-awareness during the selection of the set of swap gates – the resulted mapping of which generates the smallest critical path length (described in Section III-C). After we find a hardware-compliant mapping, we move to the next layer.

After all layers are processed, the mapping terminates.

C. Circuit Mapping Searcher

Here we describe the specific mapping searcher we use to overcome the coupling constraint for a given layer.

We build our method upon the *A-star* algorithm for finding valid mappings that minimize the number of only the inserted SWAP gates [14]. We extend it by changing the ranking metric and allowing it to search for feasible mappings that do not necessarily have the smallest SWAP gate counts. It will help us search in a way that minimizes the depth while not significantly increasing the gate count.

We rank the swap options by the increase in the critical path length. Since it is an iterative process that handles the gates layer by layer, it is tempting to consider only minimizing the depth of the already processed circuit when deciding which swaps to use.

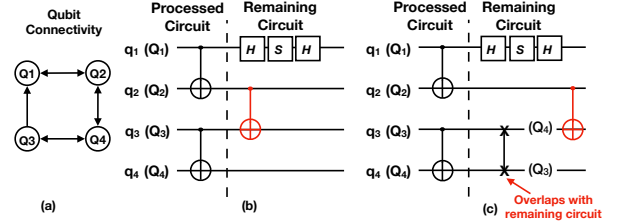


Fig. 5. (a) Layout of an example architecture with 4 physical qubits (b) Example of a quantum circuit, the dashed line separates the processed circuit and the remaining circuit (c) Inserted SWAP overlaps with remaining circuit instead of existing processed circuit

But the example in Fig. 5 shows that not only the processed circuit, but also the remaining circuit can help overlap the SWAPs with existing gates in the circuit without affecting the critical path. As shown in Fig. 5, for the CNOT gate (in red), there is no way it can overlap the necessary SWAPs with the processed circuit (dubbed as the circuit before the dashed line). But when we look after the dashed line, the three single-qubit gates can overlap with inserted SWAP. And this renders less impact to the depth of the resulting circuit, compared to if we insert the SWAP on Q_1 and Q_2 .

Based on this intuition, we design our scheme of choosing the SWAP candidate as in Fig. 6. For each of the hardware-compliant remapping candidates that we acquire from the *A-star* searcher, we calculate the critical path after merging the candidate (set of) swap(s) with both the processed circuit and the not-processed circuit. We choose the mapping that yields the shortest critical path.

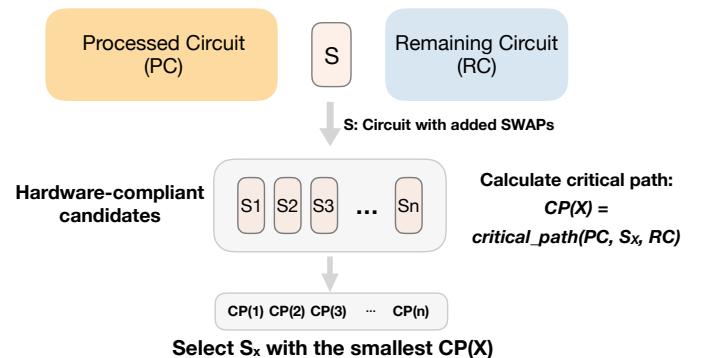


Fig. 6. Choose SWAP Candidates

D. Optimizations

We use two ways to optimize our proposed solution. One is to expand more nodes during the *A-star* search, and another one is to search into deeper levels.

1) *Expand More Nodes*: In the search process for *A-star*, the normal routine is to expand the one node of least cost at each step. Here, we can expand more than one node at each step and increase the search space. The number of nodes that can be expanded at a time can go from 1 to larger number.

2) *Deeper Search*: We increase the depth of the *A-star* search tree. In normal case, the search process ends when it finds the first node that minimizes the number of SWAPs, which is reflected as a certain level of the *A-star* tree. To this end, the second optimization that we applied here is to continue the search into a deeper level of the *A-star* tree. We can specify and tune the parameter of the deeper search.

By tuning these parameters, there are more possible nodes added into our search space. With a larger search space, we have a larger possibility to jump out of one local optima and go to the global optima.

IV. EVALUATION

In this section, we evaluate our **depth-aware swap insertion** scheme (denoted as DPS) and compare it with the two state-of-the-art qubit mappers. The experiment setup is listed below:

- **Benchmarks**: We use the quantum circuits from RevLib [20], IBM Qiskit [15], and ScaffCC [21].
- **Hardware Model**: We use IBM’s 20-qubit Q20 Tokyo architecture, which was used in [11]’s work. The qubit connectivity graph is shown in Fig. 7.
- **Evaluation Platform**: The mapping experiments are conducted on an Intel 2.4 GHz Core i5 machine, with 8 GB 1600 MHz DDR3 memory. The operating system is MacOS Mojave. We use IBM’s Qiskit [15] to evaluate the depth of the transformed circuit.
- **Baselines**: We compare our work with two best know qubit mapping solutions, the work by Zulehner and others [14] (denoted as *Zulehner*), the Sabre qubit mapper from [11] (denoted as *Sabre*), and IBM’s stochastic mapper in Qiskit. Since IBM’s Qiskit mapper is significantly worse in terms of gate count and depth than all other mappers we evaluate, as also evidenced in the work by Zulehner *et al.* [14], we do not present Qiskit results.
- **Metrics**: We are comparing the depth and gate count of the transformed circuit circuits for all different strategies.

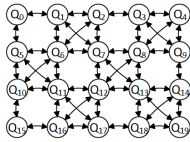


Fig. 7. IBM Q20 Tokyo Physical Layout [11]

Table. I shows a summary experimental results. For gate count, we compare the total gate count generated in the

transformed circuit. For depth, we compare the increased depth for each benchmark, denoted as “Depth-delta” in Table I. The improvement columns provides the ratio between one of the two baseline’s *depth-delta* and our *depth-delta*. We use the term *minimum improvement* to denote the improvement over the best of the two baselines, and the term *maximum improvement* to denote the improvement over the worse of the two baselines.

We discuss our findings from the following three aspects: depth reduction, gate count change, and the trade-off between gate count and depth.

A. Depth Reduction

For depth reduction, as shown in Table I, our proposed solution outperforms the two baselines *Zulehner* and *Sabre*. Comparing *depth-delta*, the added depth of the circuit, our approach outperforms the better of the two baselines by more than 20% and up to 3X. For five out of the twenty-three benchmarks, our improvement on *depth-delta* is less than 20% compared with the better of the two baselines. However, for these cases, our approach still achieves considerable improvement over the worse of the two baselines. In these cases, it is possible that one of the two baselines happen to achieve very good depth in the transformed circuit and there is not much potential to improve. But our approach is still able to find a good mapping for these benchmarks and the performance is on par with the better of the two baselines.

B. Gates Count Changes

The primary goal of our depth-aware qubit mapper is to minimize the depth of the circuit. However, we discover that our qubit mapper can sometimes reduce the gate count. We discover that four out of the twenty three (17%) benchmarks, our qubit mapper yields the smallest number of gates among all three versions of qubit mappers. For 57% of these benchmarks, our method is ranked among top-2 of the three qubit mappers in terms of gate count. For the benchmarks where our method yields the largest gate count, the increased gate count percentage is negligible. On average, our depth-aware qubit mapper adds 3% gate count. From the experiment results, we can see that our solution does not greatly increase the number of gates while reducing the depth of the circuit.

C. Trade-off between Gate Count and Depth

While all previous works focus on reducing the total gate count (and the depth among the inserted gates themselves) after qubit mapping transformation, it is crucial to think about the trade-off between the resulted gate count and depth. Sometimes the choice made during the search process that favors the reduced gate count, might adversely affect the critical path. In Table I, the *Sabre* mapper reduces the number of gates for 10-qubit QFT by 1.1% compared with *Zulehner*’s mapper, but increases the depth by 44.5%. For the *sym_9_246* benchmark, *Sabre* reduces the gate count by 3.8% compared with our approach, but increases the depth by 25.5%. Therefore a small reduction in the gate count may not be worthwhile if it increases the circuit depth significantly.

TABLE I
SUMMARY OF EXPERIMENT RESULTS

Benchmark		Total Gate #			Depth	Depth-delta			Improvement	
name	n	Zulehner	Sabre	DPS	Original	Zulehner	Sabre	DPS	Min	Max
4gt5_75	5	131	122	119	47	44	44	29	1.52	1.52
mini-alu_167	5	435	396	432	162	131	125	119	1.05	1.10
mod10_171	5	361	328	298	139	117	89	39	2.28	3
alu-v2_30	6	804	717	795	285	261	241	201	1.20	1.30
decod24-enable_126	6	533	476	509	190	187	150	141	1.06	1.33
mod5adder_127	6	849	780	858	302	256	256	222	1.15	1.15
4mod5-bdd_287	7	94	94	94	41	18	23	17	1.06	1.35
alu-bdd_288	7	126	117	135	48	36	36	30	1.2	1.2
majority_239	7	915	780	885	344	265	194	182	1.06	1.46
rd53_130	7	1619	1508	1619	569	529	482	384	1.26	1.38
rd53_135	7	419	410	422	159	116	112	109	1.03	1.06
rd53_138	8	186	183	174	56	37	40	21	1.76	1.90
cm82a_208	8	899	944	1007	337	219	295	213	1.03	1.38
qft_10	10	266	263	281	63	47	96	44	1.07	2.18
rd73_140	10	347	329	338	92	84	79	67	1.18	1.25
dc1_220	11	2868	2685	3129	1038	820	697	681	1.02	1.20
wim_266	11	1505	1415	1511	514	431	450	311	1.39	1.45
z4_268	11	4453	4477	4972	1644	1162	1492	1076	1.08	1.39
cycle10_2_110	12	9143	8666	10115	3386	2467	2640	2421	1.02	1.09
sym9_146	12	493	454	472	127	118	138	86	1.37	1.60
adr4_197	13	5299	5017	5530	1839	1439	1599	1210	1.19	1.32
rd53_311	13	467	413	446	124	138	157	87	1.59	1.80
cnt3-5_179	16	325	238	286	61	79	59	43	1.37	1.84

We compare the total gate count generated. For depth, we compare the increased depth for each benchmark, denoted as “Depth-delta” here. The improvement represents the ratio of a baseline’s depth-delta divided by DPS’s depth-delta. Min/Max represents the improvement over the best/worst baseline.

V. CONCLUSION

The physical layout of contemporary quantum devices imposes limitations for mapping a high level quantum program to the hardware. It is critical to develop an efficient qubit mapper in the NISQ era. Existing studies aim to reduce the gate count but are oblivious to the depth of the transformed circuit. This paper presents the design of the first depth-aware swap insertion scheme. Experiment results show that our proposed solution generates hardware-compliant circuits with reduced depth compared with state-of-the-art mapping schemes, with negligible overhead of increased gate count.

REFERENCES

- [1] P. W. Shor, “Algorithms for quantum computation: Discrete logarithms and factoring,” in *Proceedings 35th annual symposium on foundations of computer science*. Ieee, 1994, pp. 124–134.
- [2] L. K. Grover, “A fast quantum mechanical algorithm for database search,” in *Proceedings of the Twenty-eighth Annual ACM Symposium on Theory of Computing*, ser. STOC ’96. New York, NY, USA: ACM, 1996, pp. 212–219. [Online]. Available: <http://doi.acm.org/10.1145/237814.237866>
- [3] A. Peruzzo, J. McClean, P. Shadbolt, M.-H. Yung, X.-Q. Zhou, P. J. Love, A. Aspuru-Guzik, and J. L. OBrien, “A variational eigenvalue solver on a photonic quantum processor,” in *Nature Communications*, vol. 5, no. 1, 2014, p. 4213. [Online]. Available: <https://doi.org/10.1038/ncomms5213>
- [4] J. Preskill, “Quantum computing in the nisq era and beyond,” *Quantum*, vol. 2, p. 79, 2018.
- [5] W. Knight, “IBM Raises the Bar with a 50-Qubit Quantum Computer,” <https://www.technologyreview.com/s/609451/ibm-raises-the-bar-with-a-50-qubit-quantum-computer>, 2017.
- [6] J. Kelly, “A Preview of Bristlecone, Googles New Quantum Processor,” <https://ai.googleblog.com/2018/03/a-preview-of-bristlecone-googles-new.html>, 2018.
- [7] J. Hsu, “Intels 49-Qubit Chip Shoots for Quantum Supremacy,” <https://spectrum.ieee.org/tech-talk/computing/hardware/intels-49qubit-chip-aims-for-quantum-supremacy>, 2018.
- [8] Rigetti, <https://www.rigetti.com/>.
- [9] M. A. Nielsen and I. Chuang, “Quantum computation and quantum information,” 2002.
- [10] A. W. Cross, L. S. Bishop, S. Sheldon, P. D. Nation, and J. M. Gambetta, “Validating quantum computers using randomized model circuits,” *Physical Review A*, vol. 100, no. 3, Sep 2019. [Online]. Available: <http://dx.doi.org/10.1103/PhysRevA.100.032328>
- [11] G. Li, Y. Ding, and Y. Xie, “Tackling the qubit mapping problem for nisq-era quantum devices,” in *Proceedings of the Twenty-Fourth International Conference on Architectural Support for Programming Languages and Operating Systems*. ACM, 2019, pp. 1001–1014.
- [12] R. Wille, L. Burgholzer, and A. Zulehner, “Mapping quantum circuits to ibm qx architectures using the minimal number of swap and h operations,” in *Proceedings of the 56th Annual Design Automation Conference 2019*. ACM, 2019, p. 142.
- [13] A. Zulehner, S. Gasser, and R. Wille, “Exact global reordering for nearest neighbor quantum circuits using A*,” in *International Conference on Reversible Computation*. Springer, 2017, pp. 185–201.
- [14] A. Zulehner, A. Paler, and R. Wille, “Efficient mapping of quantum circuits to the ibm qx architectures,” in *2018 Design, Automation & Test in Europe Conference & Exhibition (DATE)*. IEEE, 2018, pp. 1135–1138.
- [15] QISKit: Open Source Quantum Information Science Kit, <https://https://qiskit.org/>.
- [16] M. Y. Siraichi, V. F. d. Santos, S. Collange, and F. M. Q. Pereira, “Qubit allocation,” in *Proceedings of the 2018 International Symposium on Code Generation and Optimization*. ACM, 2018, pp. 113–125.
- [17] S. S. Tannu and M. K. Qureshi, “Not all qubits are created equal: A case for variability-aware policies for nisq-era quantum computers,” in *Proceedings of the Twenty-Fourth International Conference on Architectural Support for Programming Languages and Operating Systems*, ser. ASPLOS ’19. New York, NY, USA: ACM, 2019, pp. 987–999. [Online]. Available: <http://doi.acm.org/10.1145/3297858.3304007>
- [18] P. Murali, J. M. Baker, A. Javadi-Abhari, F. T. Chong, and M. Martonosi, “Noise-adaptive compiler mappings for noisy intermediate-scale quantum computers,” in *Proceedings of the Twenty-Fourth International Conference on Architectural Support for Programming Languages and Operating Systems*, ser. ASPLOS ’19. New York, NY, USA: ACM, 2019, pp. 1015–1029. [Online]. Available: <http://doi.acm.org/10.1145/3297858.3304075>

- [19] A. W. Cross, L. S. Bishop, J. A. Smolin, and J. M. Gambetta, "Open quantum assembly language," *arXiv preprint arXiv:1707.03429*, 2017.
- [20] R. Wille, D. Große, L. Teuber, G. W. Dueck, and R. Drechsler, "Revlb: An online resource for reversible functions and reversible circuits," in *38th International Symposium on Multiple Valued Logic (ismvl 2008)*. IEEE, 2008, pp. 220–225.
- [21] A. JavadiAbhari, S. Patil, D. Kudrow, J. Heckey, A. Lvov, F. T. Chong, and M. Martonosi, "Scaffcc: a framework for compilation and analysis of quantum computing programs," in *Proceedings of the 11th ACM Conference on Computing Frontiers*. ACM, 2014, p. 1.